Gaining insights into the life-history strategies of tropical tree species from a large urban inventory dataset

Hao Ran Lai[a,b,*] Daniel C. Burcham[c] James Wei Wang[d]
Daniel B. Stouffer[a,e] Damien Wenjie Qiu[d] Alex Thiam Koon Yee[d]

[a] Centre for Integrative Ecology, School of Biological Sciences, University of Canterbury, Christchurch 8140, Aotearoa New Zealand

[b] Bioprotection Aotearoa, Centre of Research Excellence, Aotearoa New Zealand

[c] Department of Horticulture and Landscape Architecture, College of Agricultural Sciences, Colorado State University, Fort Collins, CO 80523, United States

[d] National Parks Board, Singapore Botanic Gardens, Singapore, Singapore

[e] Department of Evolutionary and Integrative Ecology, Leibniz Institute of Freshwater Ecology and Inland Fisheries (IGB), Berlin, Germany

[*] Corresponding email: hrlai.ecology@gmail.com

Highlights

- Trees provide ecosystem services that change dynamically with their sizes.
- We modelled diameter growth using a large tropical urban tree inventory.
- Importantly, our model contains biologically interpretable parameters.
- The growth parameters positioned species along a fast–slow continuum.
- Our model provides insightful biology in addition to accurate predictions.

Abstract

Trees are important ecosystem service providers that improve the physical environment and human experience in cities throughout the world. Since the ecosystem services and maintenance requirements of urban trees change as they grow in time, predictive models of tree growth rates are useful to forecast societal benefits and maintenance costs over a tree's lifetime. However, many models to date are phenomenological models with good prediction accuracies but lacking biologically interpretable parameters. This has limited our understanding of species life-history strategies for guiding tree species selection for urban plantings. In this study, we fit a diameter growth model to a large municipal tree inventory in Singapore using Bayesian inference along with an ordinary differential equation solver to obtain both accurate predictions and biologically interpretable parameters. We show that the 90 tree species studied here have growth parameters described by a tradeoff between fast juvenile growth when small versus slower but sustained adult growth when large, corresponding to the well-established "fast–slow" plant economics spectrum. We also use the growth model to calculate the time required to reach specific target diameters to directly illustrate a practical use case of our model inferences. Our findings highlight a more tangible way of selecting species for planting based not only on predicted growth, but also intuitive life-history growth characteristics that could be further generalised by functional traits to explore new species suitable for urban forestry.

Graphical abstract

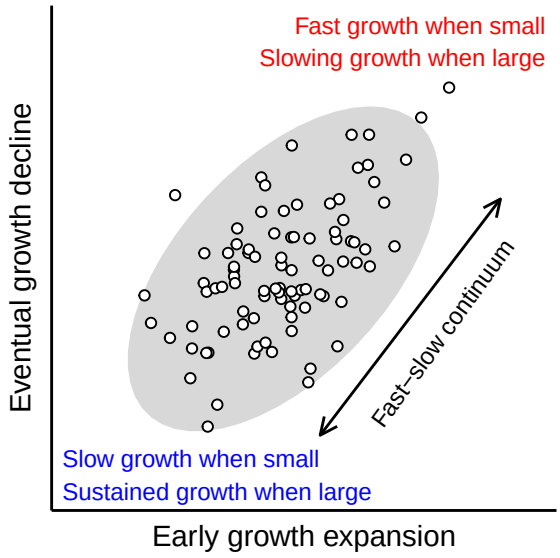

Keywords

Life-history strategy; tree demography; vital rate; ontogeny; ordinary differential equation; Singapore

Abbreviations

None.

1 Introduction

Trees play an integral role in improving the physical environment and human experience in cities (Pataki et al., 2011; Shanahan et al., 2017). In general, trees growing in urban areas require active arboricultural management to balance their social benefits (e.g., aesthetic values, heat mitigation, nature-based recreation) with potential costs (e.g., infrastructure damage, constraints on development). Urban tree management is a multi-faceted endeavour that involves both upstream planning and integration with other urban infrastructure, and downstream site management for tree growth, removal and replacement. A key aspect of this process is the

choice of tree species, which is usually based on the experience and familiarity of individual arborists with the species choices available in a given locality. The availability of municipal tree inventory datasets has made it possible to model various aspects of urban tree demography more systematically (Nowak et al., 2004; Semenzato et al., 2011), which can then objectively inform adaptive management approaches for urban forestry renewal.

Tree growth rates are a key demographic parameter for urban forests, since the ecosystem services and maintenance requirements of urban forests change as trees grow over time (Moore, 2022; Rötzer et al., 2021). For example, canopy area largely controls rainfall interception by trees and influences the amount of stormwater runoff avoided in urban areas (Dowtin et al., 2023), and the size-dependent scaling of canopy area similarly governs many other ecosystem services, such as particulate matter deposition and shading. A predictive model of tree growth rates will therefore help us to forecast provisional returns and maintenance costs over a tree's lifetime. However, many urban tree-growth studies to-date prioritise predictive accuracy of size by selecting the best out of several competing phenomenological models that are computationally less demanding, even though they lack biologically interpretable parameters (e.g., Escobedo et al., 2011; McPherson et al., 2016). As such, phenomenological models provide limited biological insights into how *future* urban plantings could be structured by the optimal selection of tree species.

On the other hand, parameter-heavy mechanistic models prioritise a good bottom-up understanding of size growth from cellular processes, such as photosynthesis and transpiration, which are then integrated into organismal growth (e.g., Falster et al., 2011; Moorcroft et al., 2001). As trees grow, their size often increases in a sigmoidal manner over long time periods, reflecting a tree's propensity for exponential growth that is progressively opposed by various aging constraints (Falster et al., 2018; Zeide, 1993). The sigmoidal trajectory of size over a tree's lifetime translates to a rate of change in size (i.e., growth rate) that is hump-shaped: accelerating when small but later decelerating (black line in Fig. 1). Our goal is to capture these biological processes in a multispecies growth model that reaches a middle ground between phenomenological curve-fitting and mechanistic complexity, by inferring species-specific growth parameters that reflect the comparative ecology of species, thus providing a quantitative evidence-base for fu-

ture species selection.

In this study, we characterise the growth characteristics of 90 tropical tree species using a predictive model with biologically interpretable parameters, which ordinate species along a life-history spectrum defined by a tradeoff between juvenile and adult growth rates. Specifically, we leverage a large municipal tree inventory in Singapore to fit size-dependent diameter growth models to repeated measurements of trunk diameter monitored over a decade. We then illustrate some uses of the inferred growth parameters to guide species selection and tree-population planning for urban forestry in terms of two key pieces of information: (1) life-history tradeoffs between growing fast when small versus sustained growth into larger sizes and; (2) time taken for a tree to reach its maximum diameter.

2 Material and methods

2.1 Tree inventory data

We analysed the data from a municipal tree inventory managed by the National Parks Board of Singapore (NParks), which contained measurements of trunk girth of 854,412 trees growing in public landscapes (i.e., parks and roadsides) throughout Singapore from a 9.5-year period between 1 January 2010 and 1 June 2019. Later between 1 January and 30 June 2023, a subset of the trees (141,922) were remeasured and we used this as an additional dataset to validate model predictions (see *Statistical inference* below for more detail). During each inspection, trunk girth was measured 1 m above ground by a professional arborist using a flexible metal measuring tape and, after rounding most of the values (~70%) to the nearest decimeter (0.1 m), recorded in the inventory. These measurements were periodically updated with, on average, 15.7-month intervals between repeated observations. Although the dataset contained tree height information in addition to tree girth, the height measurements were not used because the values were visually estimated using an ordinal scale. Trunk girth values (m) were converted to the diameter (cm) of the circular equivalent of the measured trunk shape prior to modelling.

From the whole dataset, we imposed a few selection criteria to remove data entries that were likely erroneous. Namely, we selected surviving trees at the time of data extraction (1

June 2019) and removed trees with girth below measurement precision ($<$ 0.1-m girth) or very large diameters ($>$ 300-cm diameter). As our model used species-specific parameters, we also excluded species with fewer than 1,000 individuals or modest variation in trunk diameter (range $<$ 5 cm), implying limited variation in growth. Lastly, we omitted inventory observations from members of the palm family (Arecaceae) due to the lack of secondary growth, and the hemiephiphytic strangler fig, *Ficus benjamina*, due to measurement challenges associated with its numerous, lignified column roots. The final dataset contained 390,121 trees from 90 species. For each individual tree, we limited the data to the initial and final diameter measurements (i.e., two measurements per tree) to avoid autocorrelation within tree. Although autocorrelation due to repeated measurements within each tree can be accounted by random tree effects, in our pilot analyses we found it extremely difficult to reach model convergence because numerous trees were remeasured only once (i.e., the estimation of random effects for these trees rely on single repeated inspections). Across all trees, the time interval between first and final inspections varied from one day to 9.3 years.

2.2 Diameter growth model

Many models have been developed for organismal growth, each with their own strengths and drawbacks (e.g., Hérault et al., 2011; Paine et al., 2012; Thomas et al., 2019; Tjørve and Tjørve, 2010). For this study, we sought a middle ground between mechanistic complexity and phenomenological representation of tree diameter growth, and followed the approach adopted by Zeide (1993). Zeide reviewed a number of popular phenomenological models of tree growth, starting only from those with biologically interpretable parameters, and then distilled them into a few generalised forms. All of Zeide's general model forms can be decomposed into two components: growth expansion and growth decline. In this study, we modelled the instantaneous growth rate of diameter, D, in cm per year using an equation (Zeide's "YD form", hereafter denoted as the function z) that depends only on tree size, but not tree age, since the latter is generally much harder to obtain, especially from tropical trees that lack growth rings:

$$\frac{dD}{dt} = z(D,\ a,\ b,\ c) = aD^b e^{-c(D-1)}\,. \tag{1}$$

Equation 1 includes three biologically motivated, positive-bound parameters: a, b and c. The parameter a is the growth rate at 1-cm diameter (grey dashed lines in Fig. 1), which becomes most apparent when one substitutes $D = 1$ into Equation 1. Zeide had originally wrote the last term as e^{-cD}, but we reparameterised it slightly to $e^{-c(D-1)}$ to let Equation 1 reduce to a when $D = 1$. Doing so changes the meaning of a from the more abstract "scaling factor" to the more tangible "growth rate at 1-cm diameter". Conveniently, 1 cm is also the lower size threshold of diameter measurement in some forest inventories.

The two components, D^b and $e^{-c(D-1)}$, are size-dependent autoregulatory terms that represent growth expansion and growth decline, respectively. The growth expansion term D^b (blue curve in Fig. 1) reflects the innate tendency of living bodies to grow and cells to multiply (Zeide, 2003). The diameter's exponent b encapsulates the scaling up of productive organs for the uptake of photosynthates, water, and nutrients from a given diameter. In contrast, the parameter c in the growth decline term $e^{-c(D-1)}$ (red curve in Fig. 1) captures the exponentially diminishing return of sustaining large diameters due to respiratory and overhead costs of cell maintenance, turnover and reproduction. Over a tree's lifespan, biomass build-up causes the growth decline term to eventually dominate growth expansion, thus leading to a hump-shaped growth–diameter relationship (black curve in Fig. 1), and this hump-shaped relationship naturally creates the sigmoidal diameter-over-time trajectories commonly observed in both the field (Camac et al., 2018; Hérault et al., 2011; Kohyama et al., 2015) and theoretical models (Falster et al., 2018).

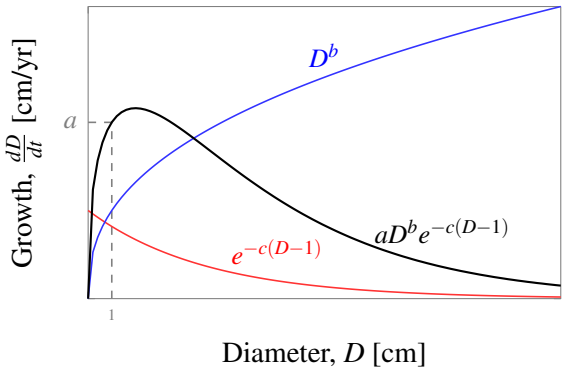

Figure 1: Conceptual diagram of a hypothetical tree species' diameter growth curve (black) given by Equation 1, which partitions the growth process into the product of two size-dependent components: growth expansion (blue) and growth decline (red).

2.3 Statistical inference

We considered several potential approaches to fit the Zeide growth model to our data. The most direct approach would be to approximate the instantaneous diameter growth rate $\frac{dD}{dt}$ using discrete-time measurements by calculating $\frac{D(t_1)-D(t_0)}{t_1-t_0}$, and then regress these calculated values against the initial diameter $D(t_0)$ (e.g., Hérault et al., 2011; Lai et al., 2022). However, there would be at least two shortcomings to such an approach. First, this approximation approach would be biased when diameters do not grow linearly over time, and in such cases the bias is particularly strong when a long time has lapsed between diameter measurements (see Fig. S1 for an illustrated example). Such an estimation bias would increase prediction error in tree sizes and size-dependent ecosystem functions. The second disadvantage of modelling discrete-time growth is related to the observation model–process model concept of Bayesian inference (Kuhnert, 2014): what we measure and observe in the field is girth or diameter, not growth. Growth is therefore a latent, unmeasurable process that ideally should be statistically *inferred* rather than calculated. In other words, the most appropriate response variable (outcome) of any regression approach is diameter, whereas growth is a process whose properties and parameters need to be inferred.

To avoid these shortcomings, we leveraged the continuous-time diameter growth model given by Equation 1 to infer instantaneous diameter growth rates by solving the corresponding ordinary differential equation. Specifically, we modelled the final diameter $D_{ij}(t_1)$ of tree i in species j at time t_1 as function of its initial diameter $D_{ij}(t_0)$, elapsed time $t_1 - t_0$, and the three growth parameters a, b and c in Equation 1 in a lognormal generalised mixed-effects model (GLMM):

$$D_{ij}(t_1) \sim \text{Lognormal}\left(\log \mu_{ij},\ \sigma_j\right),$$

where $\log \mu_{ij}$ and σ_j are the linear predictor and residual variance of final diameters in the lognormal GLMM, respectively. The predicted final diameters μ_{ij} are estimated by finding solutions to the equation

$$\int_{D_{ij}(t_0)}^{\mu_{ij}} \frac{1}{z(D_{ij},\ a_j,\ b_j,\ c_j)} dx = t_1 - t_0\,, \tag{2}$$

where the growth function z in the integral takes the nonlinear form described in Equation 1, except each growth parameter was allowed here to vary by species to account for interspecific variation: $z(D_{ij},\ a_j,\ b_j,\ c_j) = a_j D_{ij}^{b_j} e^{-c_j(D_{ij}-1)}$. The species-specific parameters (a_j, b_j and c_j) were estimated as fixed effects, i.e., without assumed correlations as in random effects. We did this to examine if any correlation between parameters would arise without prior assumption, thus providing us more confidence in concluding any tradeoff in growth strategies across species. As further elaborated in Appendix B, there is no closed-form solution for μ_{ij} in Equation 2 (i.e., the GLMM predictor cannot be conventionally written with just μ_{ij} on the left-hand side). We therefore used the built-in ODE solver `ode_rk45` in Stan to numerically calculate μ_{ij}.

Prior to model fitting, we split half of the dataset into a training set (hereafter "in-sample data") to estimate parameters, and another half into a testing set (hereafter "out-of-sample data") to validate predictions. Data splitting was performed hierarchically by species, such that each species retained 50% of its data. The model was fitted with Bayesian inference in Stan (Stan Development Team, 2023) using the `brms` package v2.19.0 (Bürkner, 2021) in R v4.2.1 (R Core Team, 2022). The custom Stan code for the ODE is available on our GitHub repository. Bayesian inference was performed with 1,000 warmup and 1,000 post-warmup Hamiltonian Monte Carlo (HMC) iterations over four chains, resulting in a total of 4,000 posterior samples. We increased the target average acceptance probability to 0.99 to promote chain convergence.

After fitting the model, we compared the residuals (difference between observed and predicted final diameters) of the in-sample data to that of the out-of-sample data to examine prediction accuracy. To further examine the ability of our model to extrapolate, we also validated the short-term forecasts on a subset of trees (52,892 individuals) that were remeasured in 2023 (four years since the last measurement in the core dataset). The 2023 predictions were made from the last measured diameter of each tree in the 2010–2019 data. That is, every tree differs in the amount of time lapsed, which ranged from 3.6 to 10.5 years.

2.4 Model applications

In addition to estimating the species-specific growth parameters a_j, b_j and c_j, we aimed to increase the utility of the model by extracting two extra pieces of information. First, we calculated the Spearman's rank correlation between the three growth parameters across the full posterior distributions as a measure of life-history tradeoff in growth strategies. For example, a strong positive correlation between two parameters indicates that species are evolutionarily or ecologically constrained to be either high or low in both growth characteristics. We chose the nonparametric rank correlation to preserve the correlation between growth parameters in both arithmetic and logarithmic scales.

Second, we calculated the passage time required for each species to reach their maximum diameter from a certain initial diameter. To begin, we set the initial diameter at 3.2 cm, or ≈ 10 cm in girth, which is a common size at which trees are transplanted into managed forests in Singapore. Next, we determined the "maximum" diameter as the diameter beyond which the growth rate is effectively zero. Because the Zeide growth model does not have a true asymptote, we opted for a slightly less arbitrary approach by setting the "practically-zero growth rate" to 0.3 cm yr^{-1}, which corresponds to the median absolute residual of our model (see *Results* and Fig. S3). The idea is that once growth rate drops below this threshold, it will be quite hard to detect any diameter increment, thus a tree is considered to have practically reached its maximum diameter. Using the full posterior distribution, we solved for the diameter value that corresponds to the eventual low growth rate of 0.3 cm yr^{-1} for each species using their inferred growth parameters and Equation 5 in Appendix C.

3 Results

Across species, our model explained 31–89% of variation (measured as Bayes R^2) in the in-sample final tree diameters; and R^2 seemed to increase with sample size (Fig. S2). In-sample and out-of-sample prediction accuracies were fairly high, both with a median residual of -0.3 cm. The residual ranges of both in- and out-of-sample predictions were also very similar: 50% of residuals fell between -2.4 and 3.1 cm, while 89% fell between -7.9 and 12.1 cm. We

consider these residuals to be reasonable given that a median-sized tree in our dataset was 22.3 cm, with an interquartile range of 12.7–44.6 cm. Increasing the time lapsed between initial and final diameter measurements did not seem to reduce prediction accuracy, as the median residuals stayed close to zero, even if the range of residuals did increase (Fig. S3). The short-term forecasts on the 2023 data also extrapolated well, with 95.0% of observations within the prediction intervals; the median residual was −0.5 cm, with 89% of residuals falling between −6.0 and 7.7 cm (Fig. S4).

The 90 species varied greatly in growth characteristics, as reflected by the three species-specific parameters a, b and c (Fig. S5). The growth parameters spanned two to three orders of magnitude, with diameter growth rate at 1 cm (a) having the greatest range (0.03–8.57 cm/yr), followed by the growth expansion factor (b, range = 0.04–4.53) and lastly the growth decline factor (c, range = 0.01–0.92). There was a strong negative correlation between a and b [Spearman's $r = -0.71$, 89% CI = (−0.78,−0.65); Fig. S5A], whereas b and c were positively correlated [$r = 0.51$, 89% CI = (0.43,0.59); Fig. S5C]. The correlation between a and c was negative but weakest of all [$r = -0.21$, 89% CI = (−0.29,−0.12); Fig. S5B].

In the following sections, we focus the on the positive correlation between the growth expansion factor b and the growth decline factor c, which are the two size-dependent parameters that provide the deepest insights into the life-history tradeoffs among species (Fig. 2). Most species were either high in both b and c, or low in both parameters. Few to none of the species were found in other regions of the b–c parameter space. The high b–high c species displayed more sigmoidal diameter trajectories over time in Fig. 3A or a more peaked growth–diameter relationship in Fig. 3B, leading to much faster growth rates when small that then decelerate rapidly. In contrast, the low b–low c species' diameter trajectories over time and growth–diameter relationships were less curved, leading to slower growth rates when small but sustaining growth rates longer into larger sizes.

The tree species also varied greatly in the estimated maximum diameter, ranging from 7 to 212 cm (Fig. S6). Similarly, the time required to reach maximum diameter for each species also varied greatly from 7 to 261 years (Fig. 4).

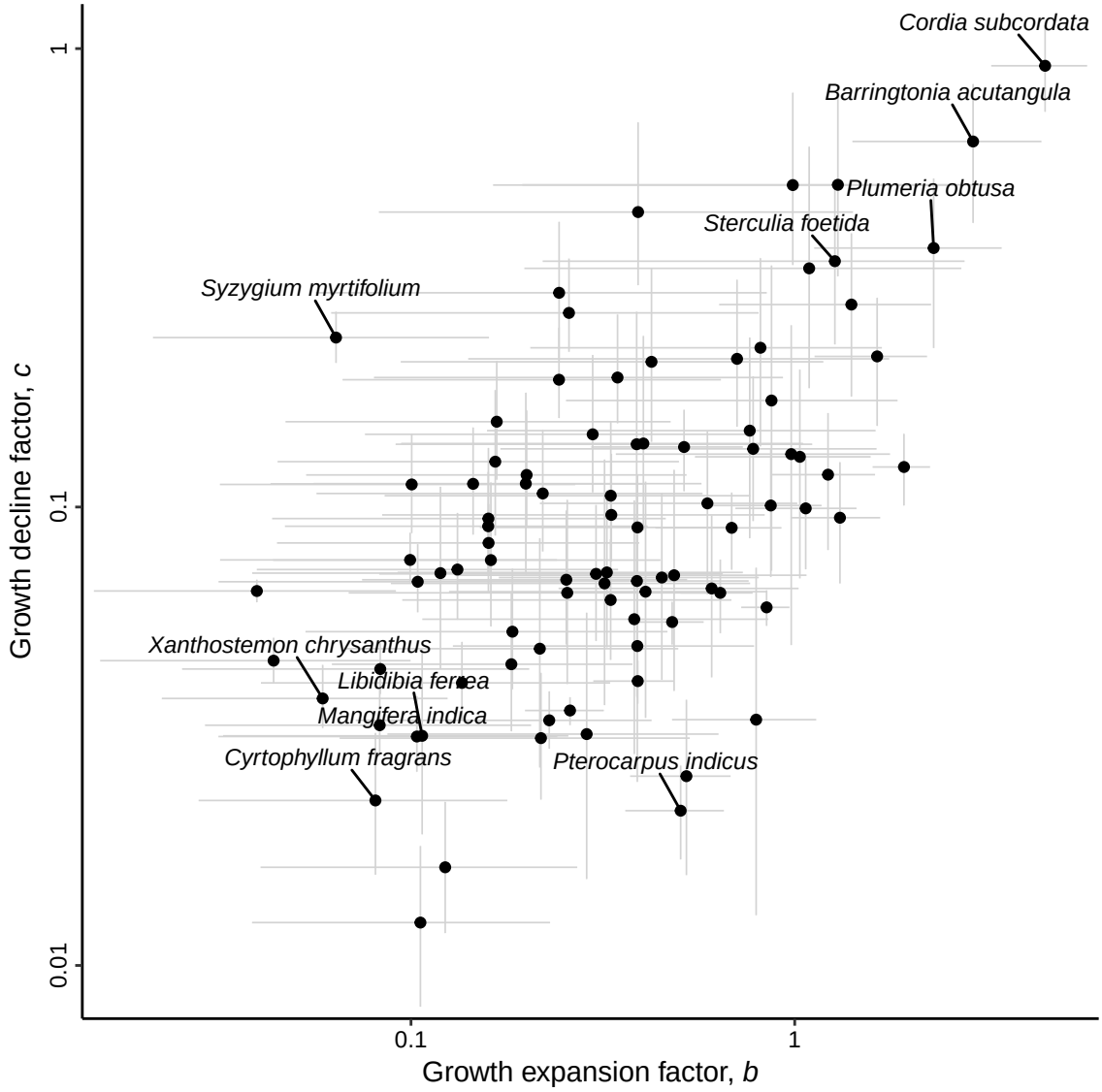

Figure 2: Life-history tradeoff in diameter growth as inferred from the correlation between the growth expansion factor, b, and the growth decline factor, c. Points and error bars are median and 89% credible intervals, respectively, of the posterior. Point size corresponds to sample size (i.e., abundance) of each species. The labelled species are examples used in the *Discussion*. Note the log-scale on both axes.

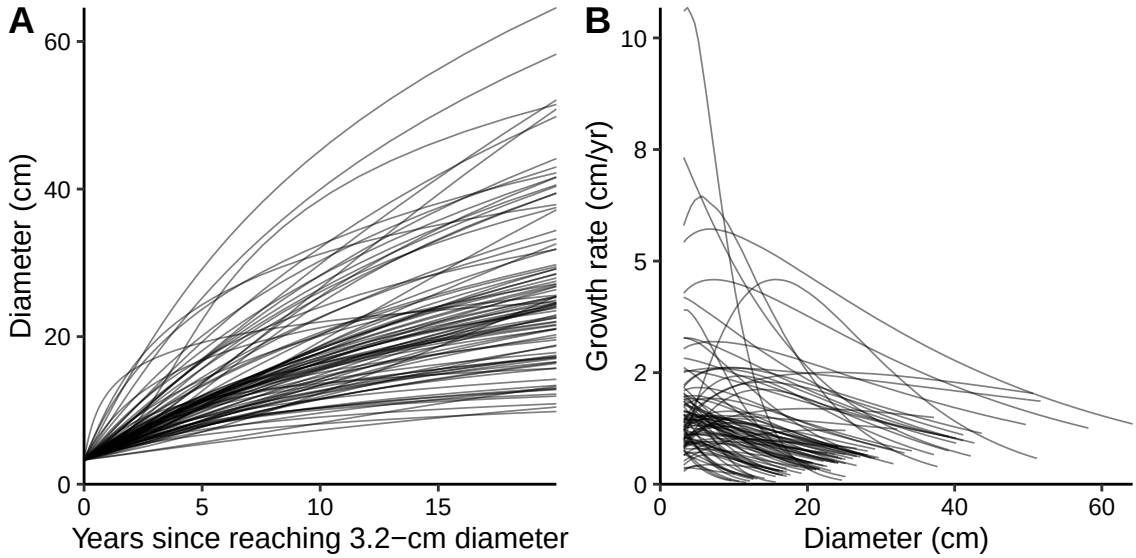

Figure 3: **(A)** Expected diameter trajectories of species from an initial diameter of 3.2 cm ($\approx$ 10 cm girth, which is a common size at planting in our study area) over 20 years. **(B)** The instantaneous growth rates (instantaneous slopes of each trajectory in **A**) in relation to diameter. Each line denotes the median posterior prediction of a species.

4 Discussion

In this study, we quantified the growth characteristics of 90 tropical tree species using an urban tree inventory dataset comparable to some of the largest existing forest inventories (e.g., Anderson-Teixeira et al., 2015; Vidal et al., 2016). Distinct from similar work in temperate climates (Schelhaas et al., 2018), it was possible to model diameter growth for many more species due to the high diversity supported by our study site's tropical environment, which facilitates a more comprehensive comparison of life-history strategies across species. We demonstrated the good prediction accuracy of our growth model, and then leveraged its biologically-interpretable parameters to compare tree growth strategies by their relative positions along the "fast–slow" plant economics spectrum (Reich, 2014) (i.e., tree species tend to either grow faster when small and then decelerate rapidly or grow slower when small but sustain growth over a longer lifespan). Such a life-history tradeoff leads to high variations among species in the temporal trajectories of diameter growth, maximum attainable diameter, and time required for each to realise those maximum diameters.

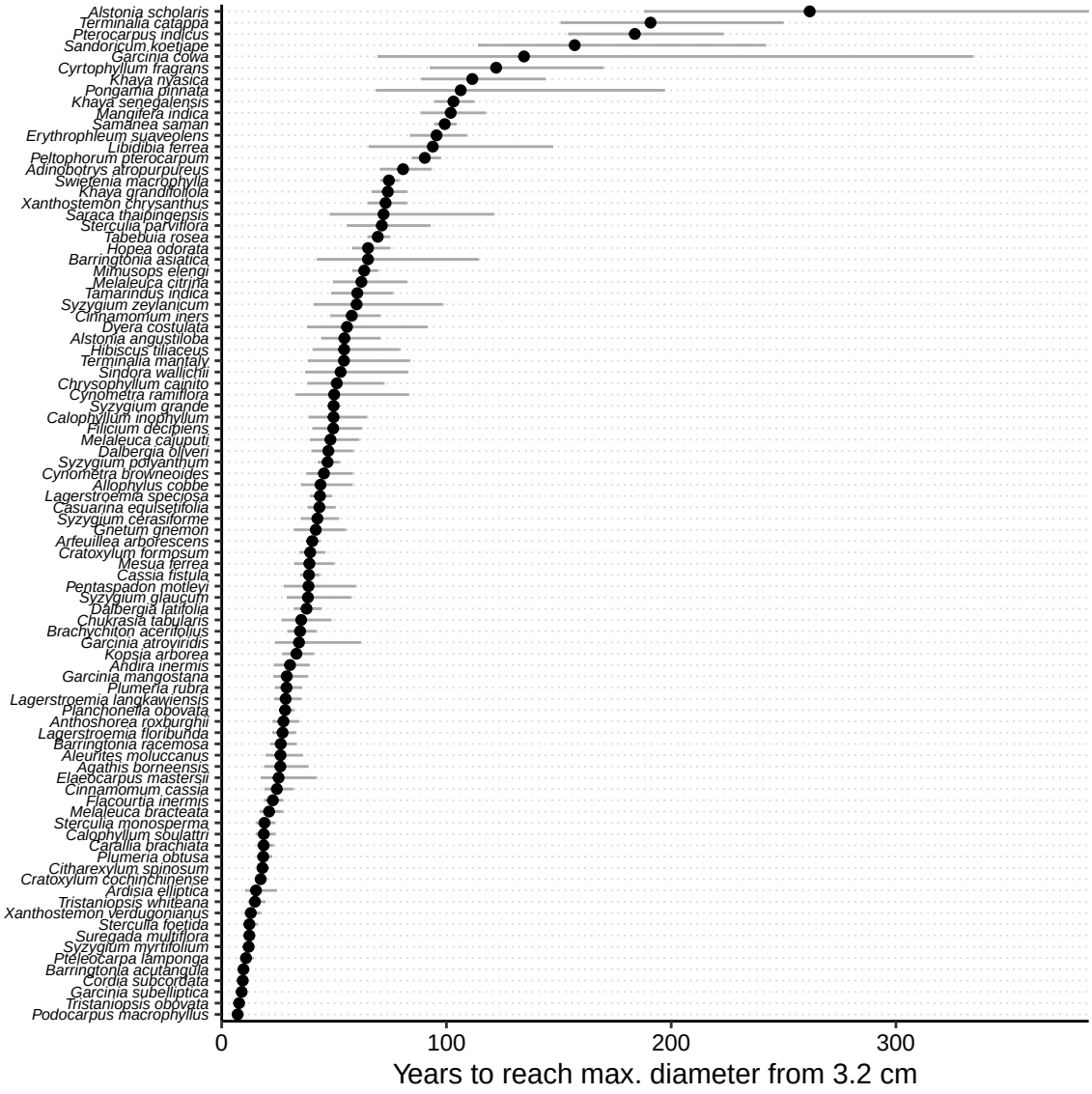

Figure 4: Years required for each species to reach its maximum diameter from an initial diameter of 3.2 cm ($\approx$ 10 cm girth, which is a common size at planting in our study area). Points and error bars are median and 89% credible intervals, respectively, of the posterior predictions.

4.1 Model performance

We first established that the fitted Zeide growth models compared favourably in terms of prediction accuracy to existing empirical models of urban tree growth models, which have reported elsewhere R^2 values around 0.5–0.9 (e.g., McPherson et al., 2016; Semenzato et al., 2011). Although a few of our species (17%) had prediction accuracies below a previously reported minimum R^2 of 0.5 (McPherson et al., 2016), we considered this a worthwhile cost relative to the benefit of deeper insights into these species' underlying biology. Furthermore, many of the previous growth models with high goodness-of-fit are polynomial equations that fit the data well within the observed diameter range but extrapolate more poorly (Song et al., 2020). In contrast, our model remained robust when predicting over longer timespans and onto large diameters (Figs S3 and S4).

Although the range of our predicted diameter growth rates overlapped with values reported for other species in natural forests (e.g., Hérault et al., 2011; Kohyama et al., 2015; Rüger et al., 2011), our trees could display growth rates up to a magnitude greater similar to the urban trees in McPherson et al. (2016). For example, a *Swietenia macrophylla* tree with a diameter of 10–20 cm was reported to grow at about 0.5 cm yr^{-1} in its native Amazonian range (Grogan et al., 2014), but the same-sized trees in our study location grew over 2.0 cm yr^{-1} on average. The main reason for the higher growth rates in our study was likely because the trees in our dataset typically grew under high-light, open conditions compared to their natural or managed forest habitats (Smith et al., 2019). Moreover, many species in our dataset originated from tropical monsoon climates with pronounced dry seasons, whereas the study location lacks an extensive dry season and would therefore be more conducive to the year-round growth of these species compared to their habitat of origin. Furthermore, unusually early peak growth rates could reflect the arboricultural practice of providing compost and supplementary irrigation during the establishment stage.

4.2 Life-history tradeoff in diameter growth

Reich (2014) posited a unified "fast–slow" plant economics spectrum, along which a trade-off exists between traits optimising growth rates under high resource availability conditions and

traits optimising survival under low resource availability conditions. Our findings support this theory with the correlation between the growth expansion factor b and the growth decline factor c (Fig. 2). The 90 tree species seemed to be constrained to either be high in both b and c (growing fast when small), or low in both (growing slow when small but sustained growth when large). Practically no species were found in the high b–low c quadrant (fast growth throughout all size classes). Moreover, our results imply a nuanced interpretation of "fast growth": species at opposite ends of the life-history spectrum (high b–high c versus low b–low c) display contrasting instantaneous diameter growth curves that cross one another over time, resulting in an ontogenetic rank swap in growth rates. The high b–high c species (e.g., *Cordia sebestena*, *Barringtonia acutangula*, *Plumeria obtusa*, *Sterculia foetida*) that grow faster when small eventually grow slower than the low b–low c species (e.g., *Cyrtophyllum fragrans*, *Libidibia ferrea*, *Mangifera indica*, *Xanthostemon chrysanthus*; Fig. 3B). Thus, species that exhibit rapid growth during early life stages tend not to sustain this growth in subsequent growth phases. These life-history tradeoffs likely reflects several biological processes, such as trees that grow fast and die fast reaching their natural mature size earlier for reproduction (Wenk and Falster, 2015), a trade-off between fast growth and tree hydraulic and mechanical safety (Eller et al., 2018), and a trade-off between intrinsic cell metabolism and deterioration in cell function (Brienen et al., 2020).

To further strengthen our mechanistic understanding, future work could identify plant functional traits that underpin such a life-history tradeoff. "Soft" functional traits that are more easily available, such as wood density, are promising promising predictors of the growth parameters (Hérault et al., 2011), whereas "hard" physiological traits that are more labour intensive to measure, such as xylem hydraulic conductivity and photosynthetic rate, provide even finer insights into how cellular functions scale to organismal growth (Falster et al., 2011; He et al., 2022; Reich, 2014). These traits can be used, for example, to test if tree species are evolutionarily restricted from having high growth expansion and low growth decline factors to always grow fast (i.e., the dearth of species in the bottom-right quadrant of Fig. 2). We showed that species with fast growth when small also have slower growth when they are large, thus attaining lower maximum sizes. Could this tradeoff be related to hydraulic traits that permit highly

energetic growth when small but constrain an upper limit on tree stature due to difficulties in transporting water to the canopy (Liu et al., 2019; Poorter et al., 2010)?

4.3 Practical uses of the growth model

Our growth model offers two potential applications for species selection in arboriculture practices. First and foremost is the direct use of growth parameters to select species with the preferred life-history characteristics for specific landscape contexts. For example, species that grow rapidly up to a relatively small mature size (high b–high c) would be suitable candidates for urban sites where it is desirable to have high foliage cover from the outset (e.g., park entrances). On the other end of the life-history spectrum, species that grow more slowly when small but show slower decline in growth rates when large (low b–low c) would be more appropriate for urban locations where the land use is expected to be more stable (e.g., heritage areas). Certain species at the peripheries of the overall growth-rate tradeoff may warrant particular attention in terms of planting strategy. For example, species showing fairly high growth rates across all size classes (low c but relative high b) are not likely to be suitable for constrained urban spaces, given their propensity for long-term growth (e.g., *Pterocarpus indicus*). Conversely, species with low growth rates overall (low b but relatively high c) would likely be suitable choices for these tight spaces (e.g., *Sygyzium myrtifolium*). More generally for urban forest management, the diameter growth rates obtained from the model would be useful to optimise planting strategy in particular sites, for example, by combining both fast-growing and slower-growing tree species to achieve shade provision over the shorter term, while sustaining the longer term needs for shade and other environmental benefits through the slower-growing species that requires less maintenance. Nevertheless, it should be acknowledged that there are other relevant factors to consider for urban trees besides growth rates, such as structural safety, habitat value for wildlife, aesthetics, native conservation status, and susceptibility to disease (Conway and Vander Vecht, 2015; Trowbridge and Bassuk, 2004).

Second, our model also allows us to calculate the number of years required for each species to attain a given diameter. This is potentially useful for grounding the expectations of public stakeholders for new development sites, or when existing sites are affected by re-development

or infrastructure works and will need to be replanted. Additionally, the models can also be used to more accurately project overall values of ecosystem services that scale directly with size (e.g., carbon sequestration and evapotranspirative cooling).

4.4 Limitations and future directions

The lower model accuracy for some species could be due to the lack of model terms accounting for the influence of exogenous factors, such as abiotic environment (e.g., climate and soil properties) and management practices (e.g., pruning and fertilization), which would have contributed to error in prediction or parameter estimations. Competitive pressure from neighbouring trees may also become an increasingly important driver of urban tree growth (Brienen and Zuidema, 2006; Schelhaas et al., 2018), and many studies have examined suitable size-dependent growth models accounting for the biotic interactions among forest trees (e.g., Lai et al., 2022; Rüger et al., 2011). Additionally, the inclusion of maintenance records containing information about the cultural practices used to care for trees will be especially useful. Accordingly, we recommend future tree growth models to include both traits and environments, as well as their interaction, as moderators of tree growth parameters.

Furthermore, it would be prudent to acknowledge the low measurement precision of data as a potential limitation of the growth model and inferences. It is important to note that most of our field measurements (~70%) were rounded to the nearest 10-cm girth ($\approx$ 3-cm diameter). This is a rather low precision compared to the range of inferred annual diameter growth rates (see Y-axis values in Fig. 3B). In addition, very large values of diameters in buttressing species, such as *Pterocarpus indicus* and *Terminalia catappa*, may be prone to further measurement error. Other than impacting parameter estimations, low measurement precision also makes model validation challenging because we cannot be sure if a mismatch between predicted and observed diameters is due to poor modelling or poor measurement, especially for slow-growing species. Despite the coarse girth measurements, our study still clearly shows the potential for scientific insights from inventory data collected primarily for management purposes. We recommend that cities use a measurement precision corresponding to smaller growth increments. Although most girth measurements in our study were rounded to the nearest decimetre, there remained some diligent

records with greater precision (rounded to the nearest centimeter), which surely have helped in the modelling process.

Although we have quantified the growth characteristics of 90 species for future plantings, practitioners may still wish to consider new species under different circumstances, for example to design a planting palette that includes more under-studied native species or one that is more tolerant to future climate change (Laughlin et al., 2018). For these applications, a good understanding of trait–demography relationships will allow us to extrapolate predictions onto new species (e.g., Hérault et al., 2011). This research direction is a promising avenue given the increased accessibility of global and regional trait databases (e.g., Falster et al., 2021; Kattge et al., 2011). Although trait-based theories of plant demography are mostly established from unmanaged forests, recent urban studies suggest that these trait–demography relationships are also generalisable to more managed settings (Simovic et al., 2024; Watkins et al., 2021).

4.5 Conclusions

We have demonstrated that it is feasible to fit models with biologically interpretable parameters to municipal tree growth records with good accuracy, thus granting insights into the comparative life histories of tree species in tropical urban landscapes. By identifying the position of species along the established fast–slow continuum, our findings provide a quantitative evidence base to select species for planting based on preferred growth characteristics. We hope that this approach will empower urban tree managers to take bolder steps to respond dynamically to diverse selection pressures on urban tree performance, backed by empirical data.

Author contributions

Hao Ran Lai: Conceptualization; Data curation; Formal analysis; Methodology; Visualization; Roles/Writing - original draft. **Daniel C. Burcham:** Conceptualization; Project administration; Roles/Writing - original draft. **James Wei Wang:** Conceptualization; Project administration; Writing - review & editing. **Daniel B. Stouffer:** Formal analysis; Writing - review & editing. **Damien Wenjie Qiu:** Conceptualization; Writing - review & editing. **Alex Thiam**

Koon Yee: Conceptualization; Funding acquisition; Writing - review & editing.

Data statement

The data that has been used is confidential. Codes for the model will be archived on GitHub/Zenodo with a DOI link upon acceptance.

Acknowledgement

We are very grateful of Daniel S. Falster who suggested the elegant "$D-1$" reparameterisation of the Zeide function, and Peter A. Vesk who reminded us of the distinction between observation model and process model. Special thanks for Daryl Lee for assisting to obtain the dataset. This work was initiated by the Centre for Urban Greenery & Ecology Research Fellowship to HRL managed by the National Parks Board of Singapore. HRL was further supported by the Royal Society Te Apārangi (Marsden grant MFP-UOC2102) and the Bioprotection Aotearoa Centre of Research Excellence.

5 References

Anderson-Teixeira, K.J., Davies, S.J., Bennett, A.C., Gonzalez-Akre, E.B., Muller-Landau, H.C., Wright, S.J., Abu Salim, K., Almeyda Zambrano, A.M., Alonso, A., Baltzer, J.L., Basset, Y., Bourg, N.A., Broadbent, E.N., Brockelman, W.Y., Bunyavejchewin, S., Burslem, D.F., Butt, N., Cao, M., Cardenas, D., Chuyong, G.B., Clay, K., Cordell, S., Dattaraja, H.S., Deng, X., Detto, M., Du, X., Duque, A., Erikson, D.L., Ewango, C.E., Fischer, G.A., Fletcher, C., Foster, R.B., Giardina, C.P., Gilbert, G.S., Gunatilleke, N., Gunatilleke, S., Hao, Z., Hargrove, W.W., Hart, T.B., Hau, B.C., He, F., Hoffman, F.M., Howe, R.W., Hubbell, S.P., Inman-Narahari, F.M., Jansen, P.A., Jiang, M., Johnson, D.J., Kanzaki, M., Kassim, A.R., Kenfack, D., Kibet, S., Kinnaird, M.F., Korte, L., Kral, K., Kumar, J., Larson, A.J., Li, Y., Li, X., Liu, S., Lum, S.K., Lutz, J.A., Ma, K., Maddalena, D.M., Makana, J.R., Malhi, Y., Marthews, T., Mat Serudin, R., McMahon,

S.M., McShea, W.J., Memiaghe, H.R., Mi, X., Mizuno, T., Morecroft, M., Myers, J.A., Novotny, V., Oliveira, A.A. de, Ong, P.S., Orwig, D.A., Ostertag, R., Ouden, J. den, Parker, G.G., Phillips, R.P., Sack, L., Sainge, M.N., Sang, W., Sri-Ngernyuang, K., Sukumar, R., Sun, I.F., Sungpalee, W., Suresh, H.S., Tan, S., Thomas, S.C., Thomas, D.W., Thompson, J., Turner, B.L., Uriarte, M., Valencia, R., Vallejo, M.I., Vicentini, A., Vrska, T., Wang, X., Wang, X., Weiblen, G., Wolf, A., Xu, H., Yap, S., Zimmerman, J., 2015. CTFS-ForestGEO: a worldwide network monitoring forests in an era of global change. Glob Chang Biol 21, 528–549. https://doi.org/10.1111/gcb.12712

Brienen, R.J.W., Caldwell, L., Duchesne, L., Voelker, S., Barichivich, J., Baliva, M., Ceccantini, G., Di Filippo, A., Helama, S., Locosselli, G.M., Lopez, L., Piovesan, G., Schöngart, J., Villalba, R., Gloor, E., 2020. Forest carbon sink neutralized by pervasive growth-lifespan trade-offs. Nature Communications 11, 1–10. https://doi.org/10.1038/s41467-020-17966-z

Brienen, R.J.W., Zuidema, P.A., 2006. The use of tree rings in tropical forest management: Projecting timber yields of four Bolivian tree species. Forest Ecology and Management 226, 256–267. https://doi.org/10.1016/j.foreco.2006.01.038

Bürkner, P.-C., 2021. Bayesian item response modeling in R with brms and Stan. Journal of Statistical Software 100, 1–54. https://doi.org/10.18637/jss.v100.i05

Camac, J.S., Condit, R., FitzJohn, R.G., McCalman, L., Steinberg, D., Westoby, M., Joseph Wright, S., Falster, D.S., 2018. Partitioning mortality into growth-dependent and growth-independent hazards across 203 tropical tree species. Proceedings of the National Academy of Sciences of the United States of America 115, 12459–12464. https://doi.org/10.1073/pnas.1721040115

Conway, T.M., Vander Vecht, J., 2015. Growing a diverse urban forest: Species selection decisions by practitioners planting and supplying trees. Landscape and Urban Planning 138, 1–10. https://doi.org/10.1016/j.landurbplan.2015.01.007

Dowtin, A.L., Cregg, B.C., Nowak, D.J., Levia, D.F., 2023. Towards optimized runoff reduction by urban tree cover: A review of key physical tree traits, site conditions, and management strategies. Landscape and Urban Planning 239, 104849. https://doi.org/10.1016/j.landurbplan.2023.104849

Eller, C.B., de V. Barros, F., R.L. Bittencourt, P., Rowland, L., Mencuccini, M., S. Oliveira, R., 2018. Xylem hydraulic safety and construction costs determine tropical tree growth. Plant Cell and Environment 41, 548–562. https://doi.org/10.1111/pce.13106

Escobedo, F.J., Kroeger, T., Wagner, J.E., 2011. Urban forests and pollution mitigation: Analyzing ecosystem services and disservices. Environ. Pollut. 159, 2078–2087.

Falster, A.D., Gallagher, R., Wenk, E., Wright, I., Indiarto, D., Andrew, S.C., Lawson, J., Allen, S., Fuchs, A., Adams, M.A., Collin, W., Alfonzetti, M., Angevin, T., Atkin, O.K., Auld, T., Baker, A., Buckton, G., Burrows, G., Caldwell, E., Camac, J., Carpenter, R., Catford, A., Cawthray, G.R., Cernusak, L.A., Chandler, G., Chapman, A.R., Cheesman, A.W., Chen, S., Choat, B., Clinton, B., Clode, P., Coleman, H., Cornwell, W.K., Cosgrove, M., Crisp, M., Cross, E., Crous, Y., Cunningham, S., Curtis, E., Daws, M.I., Degabriel, J.L., Matthew, D., Dong, N., Duan, H., Duncan, D.H., Duncan, R.P., Duretto, M., Dwyer, J.M., Edwards, C., Esperon-rodriguez, M., Evans, J.R., Everingham, S.E., Firn, J., Fonseca, C.R., French, B.J., Frood, D., Funk, J.L., Sonya, R., Ghannoum, O., Gleason, S.M., Gosper, C.R., Gray, E., Groom, P.K., Gross, C., Guerin, G., Guja, L., Hahs, A.K., Harrison, M.T., Patrick, E., Mccarthy, J.K., Meers, T., Merwe, M.V.D., Metcalfe, D., Milberg, P., Mokany, K., Moles, A.T., Moore, B.D., Moore, N., Morgan, J.W., Morris, W., Muir, A.-. nette, Munroe, S., Nicholson, Á., Nicolle, D., Nicotra, A.B., Niinemets, Ü., North, T., O'Reilly-Nugent, A., O'Sullivan, O.S., Oberle, B., Onoda, Y., Ooi, M.K.J., Osborne, C.P., Paczkowska, G., Pekin, B., Pereira, C.G., Pickering, C.-. ine, Pickup, M., Pollock, L.J., Poot, P., Powell, J.R., Power, S.A., Prentice, I.C., Prior, L., Prober, S.M., Read, J., Reynolds, V., Richards, A.E., Richardson, B., Roderick, M.L., Rosell, J.A., Rossetto, M., Rye, B., Rymer, P.D., Sams, M.A., Sanson, G., Schmidt, S., Schulze, E.-D., Sendall, K., Sinclair, S., Smith, B., Smith, R., Soper, F., Sparrow, B., Standish, R., Staples, T.L., Taseski, G., Thomas, F., Tissue, D.T., Tjoelker, M.G., Tng, D.Y.P., Tomlinson, K., Turner, N.C., Veneklaas, E., Venn, S., Vesk, P., Vlasveld, C., Vorontsova, M.S., Warren, C., Weerasinghe, L.K., Westoby, M., White, M., Williams, N., Wills, J., Wilson, P.G., Yates, C., Zanne, A.E., Kasia Ziemińska, 2021. AusTraits – a curated plant trait database for the Australian flora. Nature Scientific Data 8, 254. https://doi.org/10.1038/s41597-021-01006-6

Falster, D.S., Brannstrom, A., Dieckmann, U., Westoby, M., 2011. Influence of four major plant traits on average height, leaf-area cover, net primary productivity, and biomass density in single-species forests: A theoretical investigation. Journal of Ecology 99, 148–164. https://doi.org/10.1111/j.1365-2745.2010.01735.x

Falster, D.S., Duursma, R.A., FitzJohn, R.G., 2018. How functional traits influence plant growth and shade tolerance across the life cycle. Proceedings of the National Academy of Sciences of the United States of America 115, E6789–E6798. https://doi.org/10.1073/pnas.1714044115

Grogan, J., Landis, R.M., Free, C.M., Schulze, M.D., Lentini, M., Ashton, M.S., 2014. Big-leaf mahogany Swietenia macrophylla population dynamics and implications for sustainable management. Journal of Applied Ecology 51, 664–674. https://doi.org/10.1111/1365-2664.12210

He, P., Lian, J., Ye, Q., Liu, H., Zheng, Y., Yu, K., Zhu, S., Li, R., Yin, D., Ye, W., Wright, I.J., 2022. How do functional traits influence tree demographic properties in a subtropical monsoon forest? Functional Ecology 36, 3200–3210. https://doi.org/10.1111/1365-2435.14189

Hérault, B., Bachelot, B., Poorter, L., Rossi, V., Bongers, F., Chave, J., Paine, C.E.T., Wagner, F., Baraloto, C., 2011. Functional traits shape ontogenetic growth trajectories of rain forest tree species. Journal of Ecology 99, 1431–1440. https://doi.org/10.1111/j.1365-2745.2011.01883.x

Kattge, J., Díaz, S., Lavorel, S., Prentice, I.C., Leadley, P., Bönisch, G., Garnier, E., Westoby, M., Reich, P.B., Wright, I.J., Cornelissen, J.H.C., Violle, C., Harrison, S.P., Van Bodegom, P.M., Reichstein, M., Enquist, B.J., Soudzilovskaia, N.A., Ackerly, D.D., Anand, M., Atkin, O., Bahn, M., Baker, T.R., Baldocchi, D., Bekker, R., Blanco, C.C., Blonder, B., Bond, W.J., Bradstock, R., Bunker, D.E., Casanoves, F., Cavender-Bares, J., Chambers, J.Q., Chapin, F.S., Chave, J., Coomes, D., Cornwell, W.K., Craine, J.M., Dobrin, B.H., Duarte, L., Durka, W., Elser, J., Esser, G., Estiarte, M., Fagan, W.F., Fang, J., Fernández-Méndez, F., Fidelis, A., Finegan, B., Flores, O., Ford, H., Frank, D., Freschet, G.T., Fyllas, N.M., Gallagher, R.V., Green, W.A., Gutierrez, A.G., Hickler, T., Higgins, S.I., Hodgson, J.G.,

Jalili, A., Jansen, S., Joly, C.A., Kerkhoff, A.J., Kirkup, D., Kitajima, K., Kleyer, M., Klotz, S., Knops, J.M.H., Kramer, K., Kühn, I., Kurokawa, H., Laughlin, D., Lee, T.D., Leishman, M., Lens, F., Lenz, T., Lewis, S.L., Lloyd, J., Llusià, J., Louault, F., Ma, S., Mahecha, M.D., Manning, P., Massad, T., Medlyn, B.E., Messier, J., Moles, A.T., Müller, S.C., Nadrowski, K., Naeem, S., Niinemets, Ü., Nöllert, S., Nüske, A., Ogaya, R., Oleksyn, J., Onipchenko, V.G., Onoda, Y., Ordoñez, J., Overbeck, G., Ozinga, W.A., Patiño, S., Paula, S., Pausas, J.G., Peñuelas, J., Phillips, O.L., Pillar, V., Poorter, H., Poorter, L., Poschlod, P., Prinzing, A., Proulx, R., Rammig, A., Reinsch, S., Reu, B., Sack, L., Salgado-Negret, B., Sardans, J., Shiodera, S., Shipley, B., Siefert, A., Sosinski, E., Soussana, J.F., Swaine, E., Swenson, N., Thompson, K., Thornton, P., Waldram, M., Weiher, E., White, M., White, S., Wright, S.J., Yguel, B., Zaehle, S., Zanne, A.E., Wirth, C., 2011. TRY - a global database of plant traits. Global Change Biology 17, 2905–2935. https://doi.org/10.1111/j.1365-2486.2011.02451.x

Kohyama, T.S., Potts, M.D., Kohyama, T.I., Kassim, A.R., Ashton, P.S., 2015. Demographic Properties Shape Tree Size Distribution in a Malaysian Rain Forest. The American Naturalist 185, 367–379. https://doi.org/10.1086/679664

Kuhnert, P., 2014. Physical-statistical modelling. Environmetrics 25, 201–202. https://doi.org/10.1002/env.2276

Lai, H.R., Chong, K.Y., Yee, A.T.K., Mayfield, M.M., Stouffer, D.B., 2022. Non-additive biotic interactions improve predictions of tropical tree growth and impact community size structure. Ecology 103, e03588. https://doi.org/10.1002/ecy.3588

Laughlin, D.C., Chalmandrier, L., Joshi, C., Renton, M., Dwyer, J.M., Funk, J.L., 2018. Generating species assemblages for restoration and experimentation: A new method that can simultaneously converge on average trait values and maximize functional diversity. Methods in Ecology and Evolution 9, 1764–1771. https://doi.org/10.1111/2041-210X.13023

Lehtonen, J., 2016. The Lambert W function in ecological and evolutionary models. Methods in Ecology and Evolution 7, 1110–1118. https://doi.org/10.1111/2041-210X.12568

Liu, H., Gleason, S.M., Hao, G., Hua, L., He, P., Goldstein, G., Ye, Q., 2019. Hydraulic traits are coordinated with maximum plant height at the global scale. Science Advances 5. https://doi.org/10.1126/sciadv.aav1332

McPherson, E.G., Doorn, N. van, Peper, P.J., 2016. Urban Tree Database and Allometric Equations. General Technical Report PSW-GTR-253 86.

Moorcroft, P.R., Hurtt, G.C., Pacala, S.W., 2001. A method for scaling vegetation dynamics: The ecosystem demography model (ED). Ecological Monographs 71, 557–586. https://doi.org/10.1890/0012-9615(2001)071%5B0557:AMFSVD%5D2.0.CO;2

Moore, G.M., 2022. Lifetime cost models for large, long-lived, street trees in Australia. Arboricultural Journal 44, 21–41. https://doi.org/10.1080/03071375.2021.2014689

Nowak, D.J., Kuroda, M., Crane, D.E., 2004. Tree mortality rates and tree population projections in Baltimore, Maryland, USA. Urban Forestry and Urban Greening 2, 139–147. https://doi.org/10.1078/1618-8667-00030

Paine, C.E.T., Marthews, T.R., Vogt, D.R., Purves, D., Rees, M., Hector, A., Turnbull, L.A., 2012. How to fit nonlinear plant growth models and calculate growth rates: An update for ecologists. Methods in Ecology and Evolution 3, 245–256. https://doi.org/10.1111/j.2041-210X.2011.00155.x

Pataki, D.E., Carreiro, M.M., Cherrier, J., G., N. E., J., V., Pincetl, S., Pouyat, R.V., Whitlow, T.H., Zipperer, W.C., 2011. Coupling biogeochemical cycles in urban environments: Ecosystem services, green solutions, and misconceptions. Frontiers in Ecology and the Environment 9, 27–36.

Poorter, L., McDonald, I., Alarcón, A., Fichtler, E., Licona, J.C., Peña-Claros, M., Sterck, F., Villegas, Z., Sass-Klaassen, U., 2010. The importance of wood traits and hydraulic conductance for the performance and life history strategies of 42 rainforest tree species. New Phytologist 185, 481–492. https://doi.org/10.1111/j.1469-8137.2009.03092.x

R Core Team, 2022. R: A language and environment for statistical computing. R Foundation for Statistical Computing, Vienna, Austria.

Reich, P.B., 2014. The world-wide 'fast-slow' plant economics spectrum: A traits manifesto. Journal of Ecology 102, 275–301. https://doi.org/10.1111/1365-2745.12211

Rötzer, T., Moser-Reischl, A., Rahman, M.A., Grote, R., Pauleit, S., Pretzsch, H., 2021. Modelling urban tree growth and ecosystem services: Review and perspectives, in: Cánovas, F.M., Lüttge, U., Risueño, M.-C., Pretzsch, H. (Eds.), Progress in Botany Vol. 82. Springer

International Publishing, Cham, pp. 405–464. https://doi.org/10.1007/124_2020_46

Rüger, N., Berger, U., Hubbell, S.P., Vieilledent, G., Condit, R., 2011. Growth strategies of tropical tree species: Disentangling light and size effects. PLoS ONE 6, e25330. https://doi.org/10.1371/journal.pone.0025330

Schelhaas, M.J., Hengeveld, G.M., Heidema, N., Thürig, E., Rohner, B., Vacchiano, G., Vayreda, J., Redmond, J., Socha, J., Fridman, J., Tomter, S., Polley, H., Barreiro, S., Nabuurs, G.J., 2018. Species-specific, pan-European diameter increment models based on data of 2.3 million trees. Forest Ecosystems 5. https://doi.org/10.1186/s40663-018-0133-3

Semenzato, P., Cattaneo, D., Dainese, M., 2011. Growth prediction for five tree species in an Italian urban forest. Urban Forestry and Urban Greening 10, 169–176. https://doi.org/10.1016/j.ufug.2011.05.001

Shanahan, D.F., Cox, D.T.C., Fuller, R.A., Hancock, S., Lin, B.B., Anderson, K., Bush, R., Gaston, K.J., 2017. Variation in experiences of nature across gradients of tree cover in compact and sprawling cities. Landscape and Urban Planning 157, 231–238.

Simovic, M., Mueller, K.E., McMahon, S.M., Medeiros, J.S., 2024. Functional traits and size interact to influence growth and carbon sequestration among trees in urban greenspaces. Functional Ecology 38, 967–983. https://doi.org/10.1111/1365-2435.14505

Smith, I.A., Dearborn, V.K., Hutyra, L.R., 2019. Live fast, die young: Accelerated growth, mortality, and turnover in street trees. PLoS ONE 14, e0215846.

Song, X.P., Lai, H.R., Wijedasa, L.S., Tan, P.Y., Edwards, P.J., Richards, D.R., 2020. Height–diameter allometry for the management of city trees in the tropics. Environmental Research Letters 15, 114017. https://doi.org/10.1088/1748-9326/abbbad

Stan Development Team, 2023. RStan: The R interface to Stan.

Thomas, F.M., Yen, J.D.L., Vesk, P.A., 2019. Using functional traits to predict species growth trajectories, and cross-validation to evaluate these models for ecological prediction. Ecology and Evolution 9, 1554–1566. https://doi.org/10.1002/ece3.4693

Tjørve, E., Tjørve, K.M.C., 2010. A unified approach to the Richards-model family for use in growth analyses: Why we need only two model forms. Journal of Theoretical Biology 267, 417–425. https://doi.org/10.1016/j.jtbi.2010.09.008

Trowbridge, P.J., Bassuk, N.L., 2004. Trees in the Urban Landscape: Site Assessment, Design, and Installation. John Wiley & Sons., New York, NY.

Vidal, C., Alberdi, I.A., Mateo, L.H., Redmond, J.J. (Eds.), 2016. National Forest Inventories: Assessment of Wood Availability and Use. Springer.

Watkins, H., Hirons, A., Sjöman, H., Cameron, R., Hitchmough, J.D., 2021. Can Trait-Based Schemes Be Used to Select Species in Urban Forestry? Frontiers in Sustainable Cities 3, 1–37. https://doi.org/10.3389/frsc.2021.654618

Wenk, E.H., Falster, D.S., 2015. Quantifying and understanding reproductive allocation schedules in plants. Ecology and Evolution 5, 5521–5538. https://doi.org/10.1002/ece3.1802

Zeide, B., 2003. The U-approach to forest modeling. Canadian Journal of Forest Research 33, 480–489. https://doi.org/10.1139/x02-175

Zeide, B., 1993. Analysis of growth equations. Forest Science 39, 594–616. https://doi.org/10.1111/j.1461-0248.2006.00883.x

Appendices

A. Bias in discrete-time growth calculation

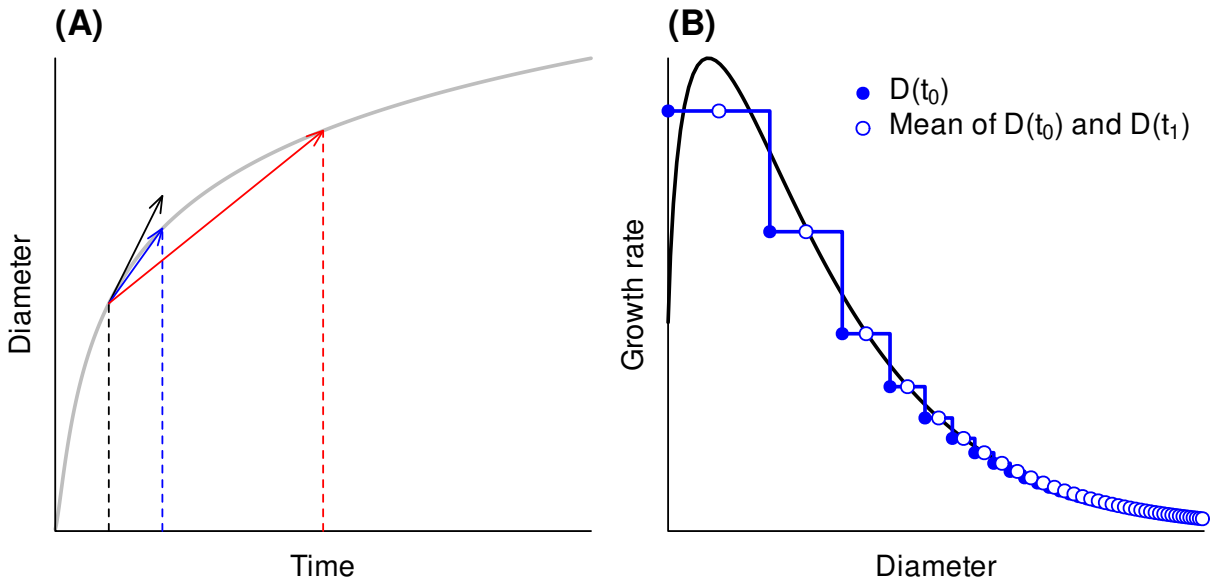

Figure S1: **(A)** Conceptual figure of potential bias in the approximation of instantaneous growth from discrete-time measurements. For a hypothetical diameter growth trajectory over time (grey curve), size-dependent diameter growth $\frac{dD}{dt}$ is the instantaneous slope at a particular diameter (black arrow, which translates to the black curve in panel **B**). Most studies, however, approximate the instantaneous growth by calculating the increment in diameter after some time interval. While such an approximation is slightly biased for short time intervals (blue), the bias becomes larger with increasing time intervals (red). In this example, discrete-time approximation of growth from a long census interval results in a considerable underestimation (red slope is much gentler than the black instantaneous slope). **(B)** Discrete approximation of instantaneous growth rate assumes a constant growth rate between census intervals (blue step-like lines), instead of a growth curve that is always adjusting to the changing diameter (black curve). When plotted or regressing against initial diameter $D(t_0)$ (a common practice in the literature), biased approximation of diameter growth from discrete measurements leads to overestimation of the instantaneous growth rate early on (blue filled circle higher than the black curve), followed quickly by underestimation later during a tree's lifespan (blue filled circle lower than the black curve). It is noteworthy that such biases can be reduced simply by plotting or regressing discrete diameter growth rates against the mean or midpoint of $D(t_0)$ and $D(t_1)$ (blue open circles), though it still is not the best approach.

B. Solving the ODE growth model to predict future diameter

Consider a generic model of instantaneous diameter growth rate of the form

$$\frac{dD}{dt} = z(D,\theta)\ , \tag{3}$$

where $z(D,\theta)$ can take any conceivable mathematical form and is a function of both current diameter D and some parameters θ. Given an initial diameter $D(t_0)$, knowledge of how much time has elapsed (i.e., $t_1 - t_0$), and the values of the parameters θ, we can mathematically determine the predicted future diameter $D(t_1)$ by integrating the dynamical Equation 3 as

$$\int_{D(t_0)}^{D(t_1)} \frac{1}{z(D,\theta)} dx = \int_{t_0}^{t_1} dt \tag{4}$$

and solving the resulting expression for the single unknown, $D(t_1)$. This is referred to as solving the model's "initial-value problem". Note that our GLMM formula (Equation 2) replaces $D(t_1)$ with μ to turn the integral from a *mathematical* expression to a *statistical* problem.

The solution to the integral on the right-hand side of Equation 4 is equal to the amount of time elapsed, $t_1 - t_0$. In contrast, the integral on the left-hand side of this equation depends on the mathematical complexity of the growth-rate model $z(D,\theta)$, and in some cases may not always be analytically tractable. When using the nonlinear form given by Equation 1, an analytical solution does indeed exist, and if we substitute this solution into Equation 4 we obtain

$$D(t_1)^{-b}\left(-cD(t_1)\right)^b \Gamma\left(1-b,-cD(t_1)\right) = ace^c\left(t_1-t_0\right) + D(t_0)^{-b}\left(-cD(t_0)\right)^b \Gamma\left(1-b,-cD(t_0)\right)\ ,$$

where $\Gamma(u,v) = \int_v^\infty x^{u-1}e^{-x}dx$ is the upper incomplete gamma function. Unfortunately, this is a transcendental equation for $D(t_1)$ in that there is no way to rearrange it and obtain a single closed-form solution for $D(t_1)$. This implies that numerical methods will need to be used to find the value of $D(t_1)$ for which the left-hand side and right-hand side of Equation 5 are equal.

C. Solving for the maximum diameter

To solve for the maximum diameter $D_{\max}$ at which a sufficiently low growth rate $\frac{dD}{dt} = \tilde{G} = 0.3$ cm yr^{-1} is reached, we could rearrange the Zeide growth model in Equation 1 to

$$D_{\max} = -\frac{b}{c}\, W\left(-\frac{c}{b}\left(\frac{e^{-c}\tilde{G}}{a}\right)^{1/b}\right), \tag{5}$$

where W is the Lambert's W function (Lehtonen, 2016), which we computed in `R` using the `lambertW` function in the `lamW` package v2.2.3. Depending on the values of a, b and c, Equation 5 could potentially have two solutions or "branches", one of which is ≤ -1 and another ≥ -1. We ensured sensible maximum diameters simply by taking the larger positive solution of the two.

D. Goodness of fit

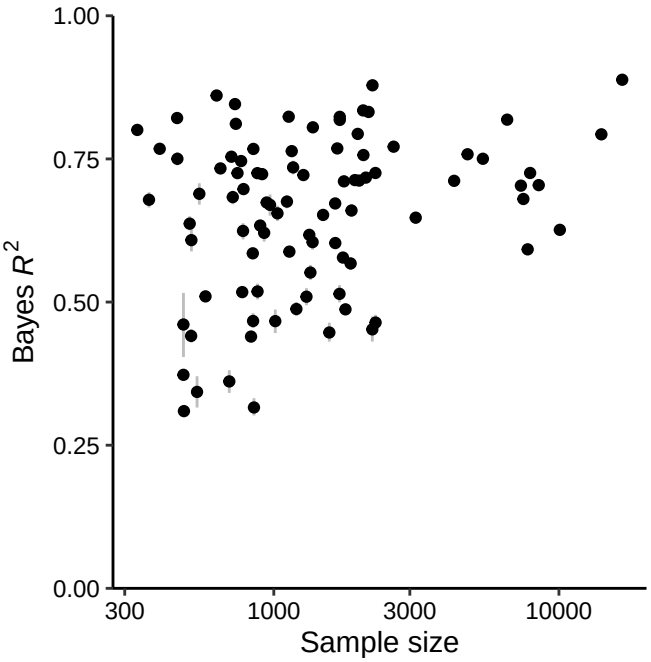

Figure S2: Bayes R^2 of each species plotted against their sample size. Points and error bars are median and 89% credible intervals (CI), respectively, of the posterior.

E. Model performance

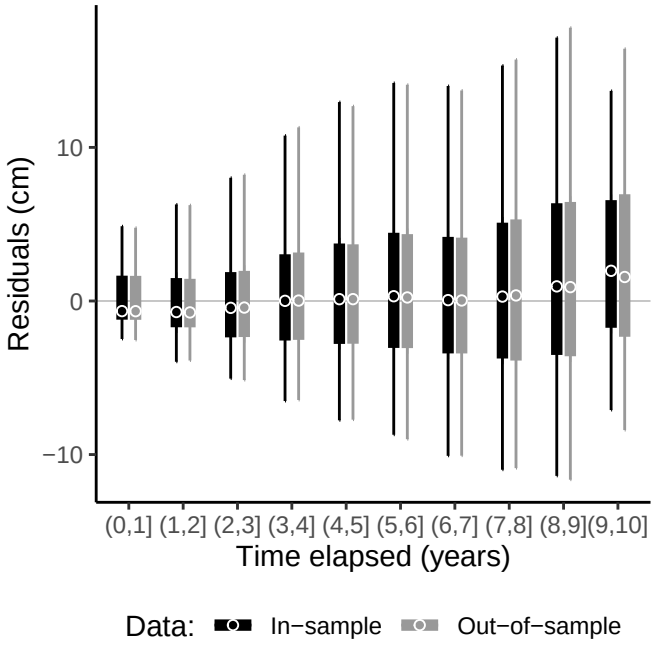

Figure S3: The relationship between residuals in diameter (i.e., observed − predicted diameter) and time lapsed between diameter measurements from in-sample (black) and out-of-sample (grey) datasets. Circles are posterior median, while thick and thick bars are 50% and 89% credible intervals, respectively.

F. Short-term forecast

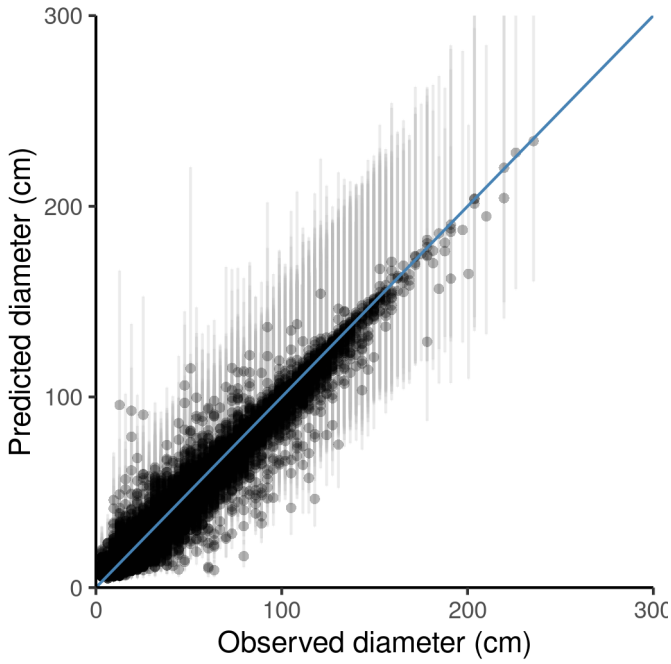

Figure S4: Validating the predicted diameter (using the model trained on 2010–2019 data) on the observed diameter of a subset of trees in 2023. The 2023 predictions were made from the last measured diameter of each tree in the 2010–2019 data, i.e., every tree differ in the amount of time lapsed. Points and error bars are median and 89% credible intervals (CI), respectively, of the posterior. Blue slope denotes the 1:1 line.

G. Pairwise comparison of all growth parameters

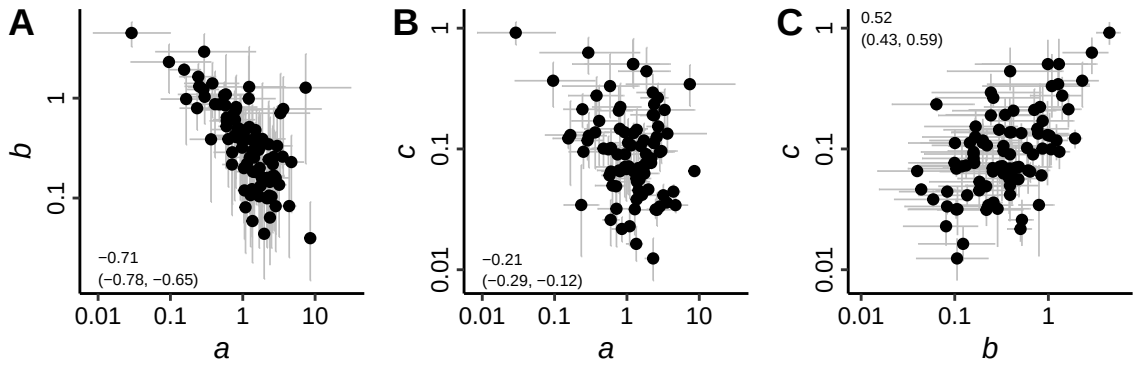

Figure S5: Pairwise comparisons of the three species-specific growth parameters: a_j (growth rate at 1-cm diameter); b_j (growth expansion factor); and c_j (growth decline factor). Points and error bars are median and 89% credible intervals (CI), respectively, of the posterior. Numbers at the corner of each panel denote the median and 89% CI of Spearman's rank correlation. Note the log-scale on both axes. Panel **C** is identical to Fig. 2.

H. Passage time in relation to maximum diameter

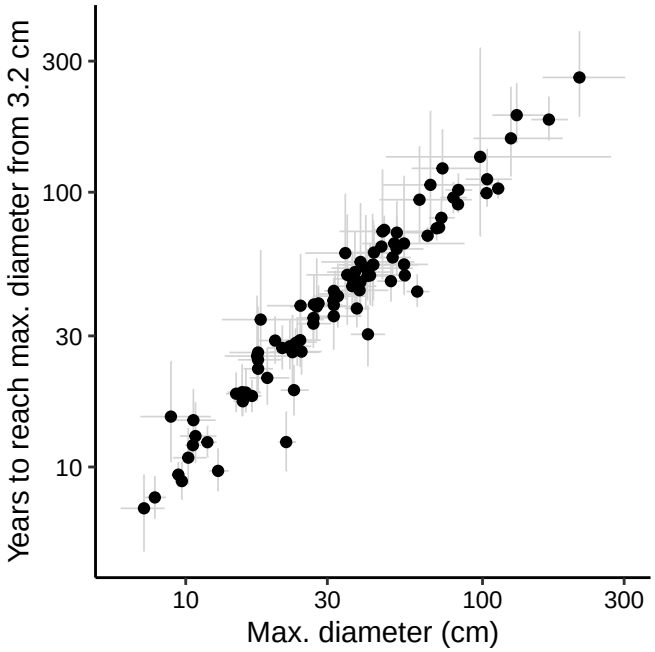

Figure S6: Relationship between maximum diameter and years to reach it from 3.2 cm ($\approx$ 10 cm girth, which is a common size at planting in our study area). Each point represents a species. Points and error bars are median and 89% credible intervals, respectively, of the posterior. The Y-axis corresponds to the X-axis in Fig. 4. Note the log-scale on both axes.